Resonance enhanced multiphoton ionisation (REMPI) and REMPI-photoelectron spectroscopy of carbonyl sulphide and carbon disulphide

Morgan, R.A.; Buma, W.J.; Baldwin, M.A.; Ascenzi, D.; Orr-Ewing, A.J.; Ashfold, M.N.R.; de Milan, J.B.; Scheper, C.R.; de Lange, C.A.

Publication date
1996

Published in
International Journal of Mass Spectrometry and Ion Processes

ELSEVIER

International Journal of Mass Spectrometry and Ion Processes 159 (1996) 1–11

International Journal of Mass Spectrometry and Ion Processes

Resonance enhanced multiphoton ionisation (REMPI) and REMPI–photoelectron spectroscopy of carbonyl sulphide and carbon disulphide

Ross A. Morgan[a], Michael A. Baldwin[a], Daniela Ascenz[1a], Andrew J. Orr-Ewing[a], Michael N. R. Ashfold[a], Wybren Jan Buma[b], Jolanda B. Milan[b], Conny R. Scheper[b], Cornelis A. de Lange[b,*]

[a]*School of Chemistry, University of Bristol, Bristol BS8 1TS, UK*
[b]*Laboratory for Physical Chemistry, University of Amsterdam, Nieuwe Achtergracht 127, 1018 WS Amsterdam, The Netherlands*

Received 15 April 1996; accepted 15 June 1996

Abstract

The results of recent mass-resolved resonance enhanced multiphoton ionisation (REMPI) and REMPI–photoelectron spectroscopy (PES) studies of the sixteen valence electron molecules OCS and CS_2 are used to illustrate some of the many opportunities offered by (and a few of the possible limitations associated with) these techniques when applied to studies of the spectroscopy and the decay dynamics of small molecules in excited electronic states.

Keywords: Resonance enhanced multiphoton ionisation; Photoelectron spectroscopy; Carbonyl sulphide; Carbon disulphide

1. Introduction

Resonance enhanced multiphoton ionisation (REMPI) spectroscopy is now recognised as a powerful technique for investigating the structure and, in favourable cases, the dynamics of the more long lived excited electronic states (e.g. Rydberg states) of small and medium sized polyatomic molecules in the gas phase [1]. Yet more information (e.g. structural data for the resulting ions and/or insight into molecular photoionization dynamics) can be gleaned when the REMPI technique is combined with kinetic energy analysis of the accompanying photoelectrons. The present work highlights recent REMPI investigations of the sixteen valence electron molecules OCS and CS_2 as a vehicle for illustrating many of these advantages. Both these molecules have linear ground states, with respective electronic configurations:

$$\text{OCS}: \ldots(6\sigma)^2(7\sigma)^2(8\sigma)^2(2\pi)^4(9\sigma)^2(3\pi)^4; \tilde{X}^1\Sigma^+ \quad (1)$$

$$\text{CS}_2: \ldots(5\sigma_g)^2(4\sigma_u)^2(6\sigma_g)^2(5\sigma_u)^2(2\pi_u)^4(2\pi_g)^4; \tilde{X}^1\Sigma_g^+$$

The electron density associated with the $2\pi_g$, highest occupied molecular orbital (HOMO) in CS_2 is distributed symmetrically, predominantly

* Corresponding author.
[1] Permanent address: Dipartimento di Chimica dell'Universita, Via Elce di Sotto, 8 1-06123 Perugia, Italy.

PII S0168-1176(96)04437-0

on the terminal atoms, whereas the corresponding (3π) orbital in OCS is concentrated at the heavy atom end. Though both HOMOs are nominally non-bonding, even a glance at the values of the wavenumbers of the three normal mode frequencies in the respective ground state neutral and the corresponding parent ions (Table 1) suffices to show that electron removal from the HOMO leads to some bond weakening. The resulting ground state ions also have linear equilibrium geometries, with $^2\Pi$ symmetry ($^2\Pi_g$ in the case of CS_2) and an inverted spin–orbit splitting. Table 2 lists values for the first three ionisation limits of each molecule and, in the case of the ground state ions, the associated spin–orbit coupling constants. The present work is concerned solely with Rydberg states of OCS and CS_2 belonging to series that converge to one or other spin–orbit component of the respective ground state ions.

The excited state spectroscopy and the photochemistry of both molecules have been much studied previously. Results up to the late 1970s have been reviewed on several occasions [2–5]. The long wavelength (290–410 nm) portion of the one-photon absorption spectrum of CS_2 contains a wealth of resolved rovibronic structure, much of which has now been assigned in terms of excitations to bent valence states arising as a result of the electronic promotion $3\pi_u \leftarrow 2\pi_g$ [6]. Proceeding to shorter wavelengths, the next feature of note is a rather intense vibronic progression spanning the region 190–210 nm; the partial analyses reported to date [7] are consistent with this being associated with excitation to the bent $^1\Sigma_u^+(3\pi_u \leftarrow 2\pi_g)$ valence state. The photochemistry of this excited state has been much studied, particularly at the ArF laser wavelength (193 nm). The current consensus [8–13] identifies contributions from both the spin-forbidden process (3) and the spin-allowed fragmentation channel (4), with the former dominant:

$$CS_2 + h\nu \rightarrow CS(X^1\Sigma^+) + S(^3P) \quad (3)$$

$$\rightarrow CS(X^1\Sigma^+) + S(^1D) \quad (4)$$

$$\rightarrow CS(a^3\Pi) + S(^3P) \quad (5)$$

Evidence to suggest that these fragmentations involve motion on more than one excited state potential energy surface come from measurements of the photofragment kinetic energies (by time-of-flight (TOF) methods) and angular distributions. The CS(X) fragments arising via dissociation pathway (3) are deduced to be highly vibrationally excited, whilst the measured recoil anisotropy parameter of the accompanying $S(^3P)$ fragments ($\beta \sim 1.0$) is consistent with absorption to the $^1\Sigma_u^+$ state then dissociation occurring after radiationless transfer to the repulsive $^3\Pi$ surface of CS_2 and retention of a near-linear geometry. The $S(^1D)$ products which are believed to arise from molecules that remain on the $^1B_2$ surface, display a more isotropic distribution of recoil velocities, consistent with the suggestion that

Table 1
Normal mode frequencies (in cm^{-1}) for OCS, OCS^+, CS_2 and CS_2^+ in their respective ground electronic states

Molecule	ν_1 (σ, C–S stretch)	ν_2 (π)	ν_3 (σ, C–O stretch)
OCS	859 [a]	520 [a]	2062 [a]
OCS^+	706 [b]	476 [b]	2075 [b]
	ν_1 (σ_g^+)	ν_2 (π_u)	ν_3 (σ_g^+)
CS_2	658 [a]	396 [a]	1535 [a]
CS_2^+	620 [c]	332 [c]	1195 [c]

[a] Ref. [2].
[b] Ref. [39].
[c] Ref. [37].

Table 2
Ionisation limits (in cm^{-1} and, in brackets, in eV) and, in the case of the X state, spin–orbit coupling constant (in cm^{-1} and, in brackets, in meV) of the ground and the first two excited states of OCS^+ and CS_2^+

	OCS	CS_2
$\tilde{X}\ ^2\Pi_{3/2}$	90210 (11.185) [a]	81286 (10.078) [b]
S–O splitting	372 (46.1) [a]	440 (54.5) [b]
$\tilde{A}\ ^2\Pi_{3/2}$	121610 (15.078) [a]	102420 (12.698) [a]
$\tilde{B}\ ^2\Sigma^+$	129390 (16.042) [a]	116760 (14.477) [a]

[a] Ref. [39].
[b] Ref. [37].

dissociation channel (4) involves a rather flat potential along the S–CS dissociation coordinate and a minimum energy pathway that suggests markedly non-linear configurations [12,13]. Price and Simpson [14] were the first to identify two Rydberg series in the vacuum ultraviolet (VUV) region, converging to the two spin–orbit components of the ground state ion; their findings have been confirmed, and extended, in later VUV absorption [15] and electron impact [16] studies. Detailed studies of the primary photochemistry of CS_2 at these shorter wavelengths remain scarce [5], but the spin-allowed channel (5) starts to contribute as soon as its energetic threshold ($\lambda \sim 158$ nm) is exceeded and is believed to dominate in the wavelength range 125–140 nm [17].

Valence excited states of OCS have also been investigated by conventional absorption spectroscopy but, in contrast to the longest wavelength features in the CS_2 spectrum, all of the associated electronic absorptions appear diffuse, namely the continua centred around 222 nm, 167 nm and 152 nm, assigned in terms of $^1\Delta \leftarrow \tilde{X}^1\Sigma^+(4\pi \leftarrow 3\pi)$, $^1\Pi \leftarrow \tilde{X}^1\Sigma^+(10\sigma \leftarrow 3\pi)$, and $^1\Sigma^+ \leftarrow \tilde{X}^1\Sigma^+(4\pi \leftarrow 3\pi)$ transitions, respectively [2–4,18–21]. The temperature dependence of the longest wavelength absorption profile [22] led to the proposal that the $^1\Delta$ excited state has a bent equilibrium geometry—a result supported by more recent studies of the energy disposal and vector correlations amongst the primary (CO(X) + S(^{1}D)) photodissociation products [23]. The 152 nm absorption shows diffuse vibronic structure (spacing ca. 800 cm^{-1}), attributable to an unstable periodic orbit on the excited $^1\Sigma^+$ surface [24]. Photodissociation within this band yields, predominantly, CO(X) + S(^{1}S) products [25] with an anisotropy parameter ($\beta \sim 1.8$, measured at 157 nm [26]) fully consistent with rather prompt dissociation following excitation via a parallel transition. The OCS absorption spectrum at shorter wavelengths is dominated by transitions to Rydberg states. The 70 000–75 000 cm^{-1} region has been studied extensively, both by one-photon absorption spectroscopy [2–4,18–20] and by electron energy loss spectroscopy [21].

Excited states of both molecules have also been investigated via the resonance enhancements they provide in the respective multiphoton ionisation (MPI) spectra. In the case of OCS, Yang et al. [27] identified two-photon resonances associated with three Rydberg states in the 70 000–75 000 cm^{-1} region: the $\tilde{E}$ and $\tilde{F}$ states, both of which, following Kopp [19], they labelled as having $^1\Pi$ symmetry, and the so-called $\tilde{P}$ state. This same region has been further investigated by Weinkauf and Boesl [28] and ourselves [29], both of whom combined one-colour 2 + 1 and 3 + 1 MPI spectroscopy with careful measurements of the kinetic energies of the accompanying photoelectrons. The former workers [28] identified five Rydberg states, all attributable to the electron promotion $4p\lambda \leftarrow 3\pi$, and suggested a number of revisions of earlier analyses [3,27]. Our more recent work [29] has succeeded in identifying a further twenty-one Rydberg origins, all of which we assign to series converging to one or other of the spin–orbit components of the ground state ion. These origins are observed to partition into clumps with associated quantum defects ca. 3.5 and 4.5 (which we assign in terms of the respective orbital promotions $5p\lambda \leftarrow 3\pi$ and $6p\lambda \leftarrow 3\pi$), and others with near-integer quantum defect which we interpret in terms of excitation to s, d and (possibly) f Rydberg orbitals.

The first multiphoton studies of the excited states of CS_2 have appeared only recently, despite the fact that it is for centrosymmetric systems like CS_2 that two-photon studies should be most rewarding [1]. One-photon parity and angular momentum selection rules dictate that the only Rydberg states of CS_2, converging upon the ground state of the CS_2^+ ion, accessible via a dipole allowed excitation from the $\tilde{X}^1\Sigma_g^+$ ground state are those derived from configurations involving the $^2\Pi_g$ ion core and an ungerade (e.g. p) Rydberg electron; it is generally accepted that the dominant series observed in the early

absorption work is associated with the $[^2\Pi_g]np\sigma_u$ configuration [14,15]. Two-photon excitations, in contrast, offer the possibility of populating Rydberg states involving gerade Rydberg orbitals, e.g. those associated with the configurations $[^2\Pi_g]ns\sigma_g$, $[^2\Pi_g]nd\sigma_g$, $[^2\Pi_g]nd\pi_g$ and $[^2\Pi_g]nd\delta_g$. Consistent with such expectations, Couris et al. [30] reported a 2 + 1 REMPI study of the 54 000–58 000 cm^{-1} energy region and identified resonances due to the two states (derived from the two spin–orbit states of the ion core) associated with the excited configuration $[^2\Pi_g]4s\sigma_g$, whilst more recent work from our own groups [31] has revealed higher energy origins with near-zero quantum defects assignable in terms of higher members of the $[^2\Pi_g]ns\sigma_g \leftarrow \tilde{X}$ and/or $[^2\Pi_g]nd_g \leftarrow \tilde{X}$ Rydberg series. Li et al. [32] and Baker et al. [33,34] have investigated the 62 000–65 000 cm^{-1} energy region using both one-colour 3 + 1 and two-colour (1 + 1′) + 1 REMPI spectroscopy and identified excited states derived from the Rydberg configuration $[^2\Pi_g]4p\lambda_u$. Our own REMPI and REMPI–PES studies [31] have served to confirm and/or refine the earlier assignments, and revealed an extensive Rydberg series based on the Rydberg configuration $[^2\Pi_g]nf_u$. In this regard, CS_2 shows quite striking similarities with CO_2, for which recent 3 + 1 REMPI and REMPI–PES studies have also revealed a series of spin–orbit split resonances associated with the configuration $[^2\Pi_g]nf_u$ (n = 4–13) [35,36].

Here we highlight a number of key features to emerge from the first comprehensive studies of the entire two- and three-photon REMPI spectra of jet-cooled samples of CS_2 and OCS up to their respective first ionisation limits. Numerous vibronic features are apparent in each spectrum the majority of which can be assigned (with the aid of concurrent measurements of the kinetic energies of the photoelectrons accompanying the REMPI process) as members of well defined Rydberg series converging to the two spin–orbit components of the respective ionic ground states [29,31]. The present work also serves to illustrate the benefits of mass-resolved REMPI spectroscopy, especially when it comes to identifying spectral features associated with photofragments rather than the parent molecule itself.

2. Experimental

The results described in this work were obtained using two complementary experimental set-ups: in Bristol, a home-built time-of-flight (TOF) mass spectrometer was used to record mass-resolved REMPI spectra of OCS, CS_2 and fragments arising from their photodissociation, whilst in Amsterdam REMPI–PES studies were performed using a "magnetic bottle" spectrometer.

Both experiments have been described previously and readers are referred to earlier publications [29,31] for a description of the apparatus and procedures.

3. Results and discussion

In this section we aim to demonstrate the merits, and some of the limitations, of the REMPI technique using recent results involving the molecules CS_2 and OCS as examples. Fig. 1 shows the mass-resolved 3 + 1 REMPI spectrum (monitoring just parent ions with m/z 76) of jet-cooled CS_2 recorded using linearly polarised laser radiation in the range 485–465 nm. This spectrum was measured using two laser dyes (coumarins 480 and 460, respectively). We have not taken any particular care about normalising the laser power within the tuning range of either dye, nor between the two dyes, so our focus here is necessarily on the frequencies of the various resonances rather than the absolute peak intensities. From this spectrum alone it is not possible to offer unambiguous assignments for the various observed resonances but, with the aid of REMPI–PES and other considerations, it is possible to deduce the vibronic character, the

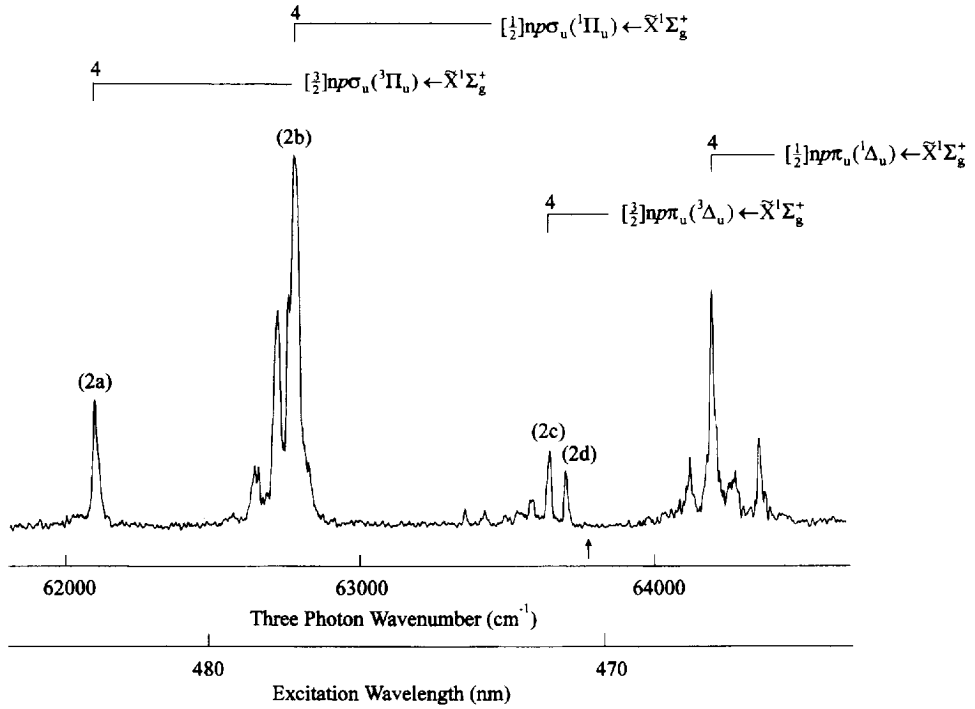

Fig. 1. 3 + 1 REMPI spectrum of a jet-cooled sample of CS_2 over the energy range 61 850–64 500 cm^{-1} recorded using linearly polarised light and monitoring only those ions with TOFs appropriate to *m/z* 76. This spectrum is a composite, obtained by splicing together spectra recorded using two different dyes. As discussed in the text, no effort was made to ensure correct normalisation of the relative intensities of features appearing within the tuning range of either dye, nor between the one dye tuning curve and the other. The vertical arrow positioned below the spectrum indicates where the two scans have been joined. Four members of the $[^2\Pi_g]4p\lambda_u \leftarrow \tilde{X}^1\Sigma_g^+$ Rydberg complex are indicated via the combs superimposed above the spectrum. REMPI–PES spectra taken at wavelengths corresponding to the peaks labelled 2a–2d are displayed in Fig. 2.

ion core configuration and, often, the symmetry of the resonance enhancing levels.

3.1. Photoelectron kinetic energy analysis

Fig. 2 shows REMPI–PE spectra associated with four of these peaks, each of which arises as a result of a three-photon resonant, four-photon ionisation process. The first REMPI–PE spectrum (Fig. 2(a)), obtained following excitation at 483.1 nm ($3\tilde{\nu}$ = 62 100 cm^{-1}), shows one dominant peak centred at a kinetic energy of 0.188 eV. Given a value of 81 286 ± 5 cm^{-1} (10.078 eV) for the first ionisation limit in CS_2 [37], energy conservation arguments dictate that the final one-photon ionisation step yields CS_2^+ ions in the ground (i.e. $v_1^+ = v_2^+ = v_3^+ = 0$) vibrational level of the lower, $^2\Pi_{3/2,g}$ (henceforth written simply as $[^3/_2]$), spin–orbit state of the ion. We then use Franck–Condon arguments, allied with the simple appearance of the spectrum, to deduce that the level providing the resonance enhancement is an electronic origin of a state (most probably a Rydberg state) with an equilibrium geometry very similar to that of the ground state ion and having a (predominantly) $[^3/_2]$ ion core. Such a conclusion is entirely consistent with that suggested in a number of previous analyses [15,33]; namely, that this feature should be assigned as the origin of the $[^3/_2]4p\sigma_u$, $(^3\Pi_u) \leftarrow \tilde{X}^1\Sigma_g^+$ Rydberg transition. The REMPI feature appearing at an excitation wavelength of 477.9 nm ($3\ \tilde{\nu}$ = 62 780 cm^{-1}) is associated with the PE spectrum shown in Fig. 2(b). In this case

the major peak appears at a kinetic energy of 0.246 eV, suggesting that ionisation results in formation of vibrationless (i.e. $v^+ = 0$) ions with a $^2\Pi_{1/2,g}$ (henceforth written simply as $[^1/_2]$) spin–orbit core. Such a result, together with the observed energy separation between this REMPI peak and the feature appearing at 62 100 cm^{-1}, encourages assignment of the 62 780 cm^{-1} resonance as the origin of the $[^1/_2]4p\sigma_u,(^1\Pi_u) \leftarrow \tilde{X}^1\Sigma_g^+$ Rydberg transition [31,33,34]. However, closer inspection of this REMPI–PE spectrum suggests that this cannot the whole story, since it does not account for the second feature, appearing at a kinetic energy of ca. 0.214 eV. Simple energetic considerations suggest that this could be associated with formation of ions in their ground, $[^3/_2]$, spin–orbit state carrying some 650 cm^{-1} of internal energy, or with spin–orbit excited ions with ca. 210 cm^{-1} of internal energy. Recalling Table 1, we see the former explanation to be the more plausible and conclude that this slower peak is indicative of the production of ground state ions with one quantum of vibration in the symmetric stretching mode (or, possibly, two quanta of bend). This, in turn, suggests some resonance enhancement at 62 780 cm^{-1} by a level of a Rydberg state carrying such vibrational excitation, i.e. most probably by the $v_1 = 1$ level of the previously discussed $[^3/_2]4p\sigma_u,(^3\Pi_u)$ state, which is located at 62 720 cm^{-1} [31].

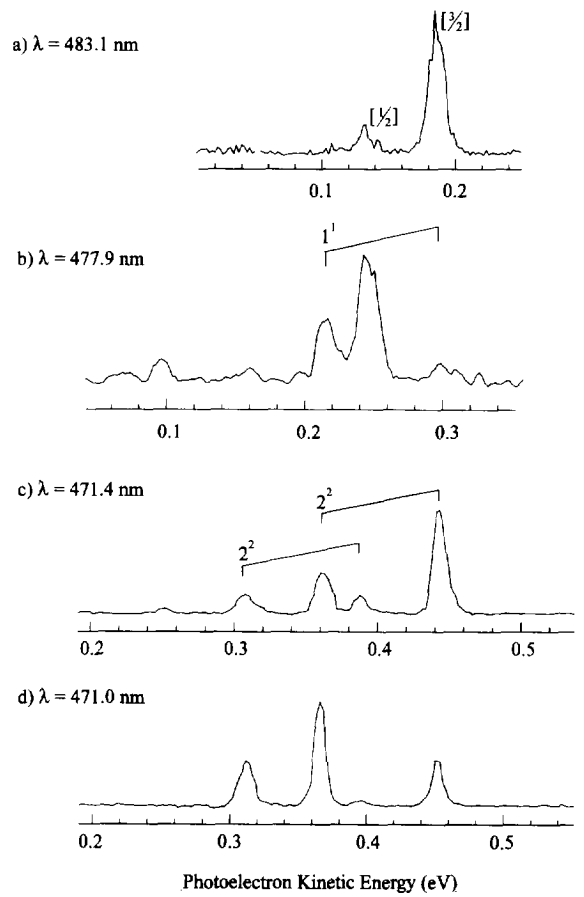

Fig. 2. Illustrative REMPI–PE spectra of CS_2 obtained following excitation at: (a) 483.1 nm, where we excite a three-photon resonance ($3\tilde{\nu}$ = 62 100 cm^{-1}) involving the origin of the $[^3/_2]4p\pi_u,(^3\Pi_u)$ Rydberg state, (b) 477.9 nm ($3\tilde{\nu}$ = 62 780 cm^{-1}), where the kinetic energy of the dominant photoelectron peak indicates that the partner ion is formed in the ground ($v^+ = 0$) level of the upper $[^1/_2]$ spin–orbit state consistent with the major resonance enhancement being provided by the $[^1/_2]4p\pi_u,(^1\Pi_u)$ Rydberg origin; (c) 471.4 nm ($3\tilde{\nu}$ = 63 644 cm^{-1}) and (d) 471.0 nm ($3\tilde{\nu}$ = 63 700 cm^{-1})—resonances which are believed to result from vibronic mixing between two states which, in zero-order, would be described as the $[^3/_2]4p\pi_u,(^3\Delta_u)$ Rydberg origin and the $^3\Delta_u$ vibronic component of the 2^2 vibrational level associated with the $[^3/_2]4p\pi_u,(^3\Sigma_u^-)$ state [31]. The kinetic energy scales have been offset so that the various vibronic states of the ion align vertically.

Not all of the resonance-enhancing levels ionise so "cleanly" as the two discussed thus far. Consider, for example, the features appearing at 471.4 nm and 471.0 nm ($3\tilde{\nu}$ = 63 644 cm^{-1} and 63 700 cm^{-1}, respectively), both of which have, on occasion, been tentatively assigned in terms of the $[^3/_2]4p\pi_u,(^3\Delta_u) \leftarrow \tilde{X}^1\Sigma_g^+$ origin transition [33,34]. The associated REMPI–PES spectra, shown in Fig. 2(c) and 2(d), suggest a solution to the existing ambiguity. The former spectrum shows four peaks, the largest of which appears at a kinetic energy (0.443 eV) consistent with ionisation to the $[^3/_2]$, $v^+ = 0$ level. Ionisation to the $[^1/_2]$, $v^+ = 0$ level (associated kinetic energy, 0.388 eV) is seen to occur with only low probability, consistent with the premise that the intermediate Rydberg state has a reasonably pure $[^3/_2]$ ion core. What then should we make of the two additional peaks at 0.360 eV and 0.306 eV which, on energetic grounds, we associate with formation of ions with both $[^3/_2]$ and $[^1/_2]$ cores, each

with ca. 650 cm^{-1} of internal energy? The PE spectrum resulting from 3 + 1 REMPI via the neighbouring 63 700 cm^{-1} feature (Fig. 2(d)) exhibits the same peaks, but the relative intensities of the "fast" and "slow" kinetic energy features are reversed. This has been explained [31] by assuming that the 63 644 cm^{-1} and 63 700 cm^{-1} resonances are the result of vibronic mixing between two levels which, in zero-order, should be viewed as (i) an electronic origin involving the $[^3/_2]$ ion core (the aforementioned $[^3/_2]4p\pi_u,(^3\Delta_u)$ origin), and (ii) an excited vibrational level of a state (most probably the $[^2\Pi_g]4p\pi_u$, $(^3\Sigma_u^-)$ state) involving a spin–orbit "mixed" core. Note that the REMPI–PE spectra provide a powerful means of establishing whether a particular resonance involves an electronic origin or a vibrationally excited level, and that (as here) the resolution will often be sufficient to allow identification of the particular spin–orbit component to which ionisation takes place. Actually assigning the excited state responsible for the resonance enhancement still requires additional information, however. Factors that have been considered [31] in reaching the assignments offered here include (i) the quantum defects of the various origins, and (ii), when attempting to distinguish Π_u and Δ_u resonances, similarities (or otherwise) with the one-photon absorption spectrum.

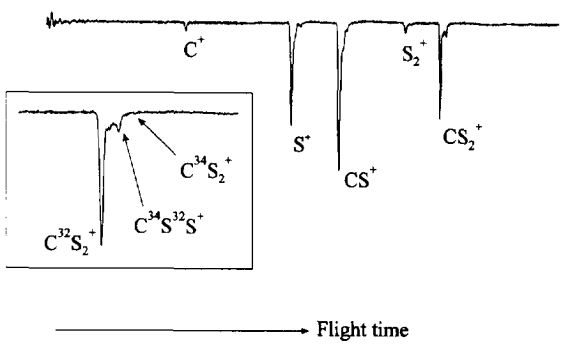

Fig. 3. Ion TOF spectrum obtained following REMPI of CS_2 at 301.5 nm using a laser pulse energy of ca. 1mJ. The inset illustrates TOF peaks associated with parent ions containing one and two ^{34}S nuclei.

3.2. Ion mass analysis

Another major asset of the REMPI technique, when applied to molecules in a jet, is the facility to mass discriminate the various ions produced. Fig. 3 shows the TOF spectrum of the ions resulting from REMPI of a jet-cooled sample of CS_2 using ca. 1 mJ pulses of 301.5 nm radiation. This clearly shows not just the parent peak (*m/z* 76), but also fragment ion peaks at *m/z* 64 (due to the S_2^+ ion), 44 (CS^+), 32 (S^+) and 12 (C^+). The extent of ion fragmentation is generally observed to increase with decreasing excitation wavelength and/or increasing pulse energies. As the inset to Fig. 3 shows, careful inspection of the parent ion peak reveals small features attributable to CS_2 molecules in which one, or both, of the sulphur atoms are the ^{34}S isotope (natural abundance 4.2%). In the case of OCS, Weinkauf and Boesl [28] used the isotope shifts between related features in the 2 + 1 REMPI spectra of $O^{12}C^{32}S$ (*m/z* 60, 94.7% natural abundance), $O^{13}C^{32}S$ (*m/z* 61, 1.1%) and $O^{12}C^{34}S$ molecules (*m/z* 62, 4.2%) as an alternative route to distinguishing electronic origins from vibronically excited bands.

As Fig. 4 shows, in the context of a prototypical

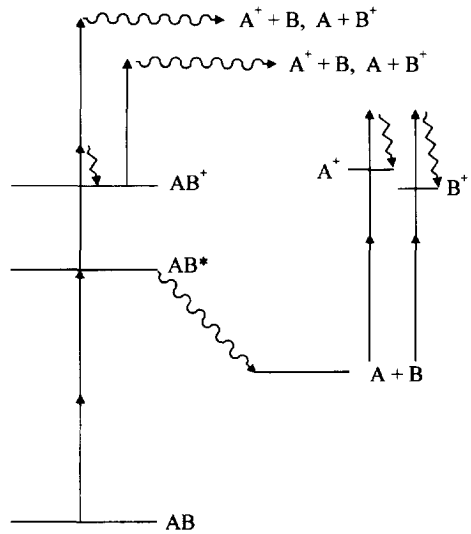

Fig. 4. Illustration of various routes to fragment ions in the REMPI of a prototypical molecule AB. ∿∿→ indicates fragmentation, and ⇝ ionisation.

molecule AB, A^+ and/or B^+ fragment ions can arise via a number of different mechanisms. Two, at least, involve multiphoton excitation of the neutral molecule to energies above the ionisation limit at which point the molecule might undergo dissociative ionisation or, alternatively, form stable parent ions which themselves dissociate following absorption of one or more additional photons. In principle photoelectron spectroscopy should be able to make a distinction between the two mechanisms, although it should be noted that dissociative photoionisation in general gives rise to a broad distribution of photoelectron kinetic energies. The fragment ions evident in the particular TOF spectrum shown in Fig. 3 are believed to arise via this latter mechanism. Since this paper is primarily concerned with the spectroscopy of the excited neutral molecule the key point of similarity that needs emphasising when considering both of these mechanisms is that the fragmentation occurs above the ionisation limit, after resonance enhancement; the excitation spectra for forming the various fragment ions should mimic that for forming the parent ion, and yield spectral data pertaining to the excited neutral AB^*. Contrast this with the case that the excited AB^* molecules fragment to yield ground (or excited) state neutral fragments. If this occurs within the timescale of the laser pulse then these fragments may themselves undergo REMPI and provide additional, wavelength-dependent, contributions to the total

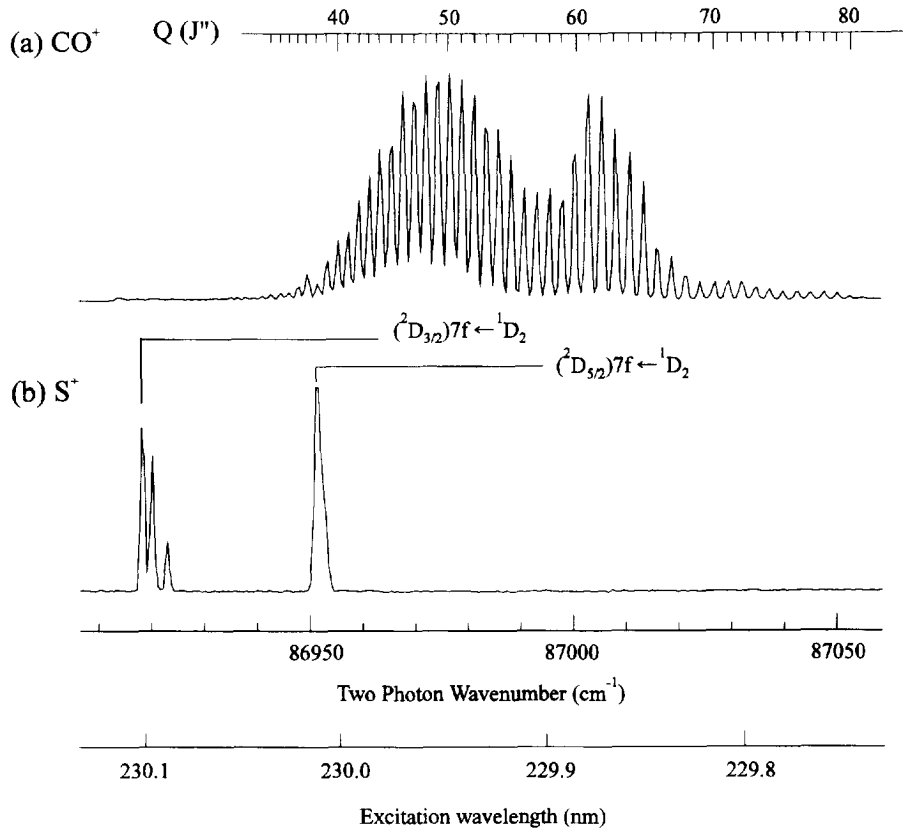

Fig. 5. 2 + 1 REMPI spectra showing (a) the Q branch of the (0,0) band of the $B^1\Sigma^+ \leftarrow X^1\Sigma^+$ transition of the CO fragments and (b) various resonances of the S(^{1}D) fragments formed by one-photon dissociation of a jet-cooled sample of OCS at the same excitation wavelength. The comb arranged over the former spectrum serves to highlight the highly inverted, bimodal rotational state population distribution of the former fragments.

ion (and total photoelectron) yield. Mass and/or electron kinetic energy analysis will be necessary to separate these various contributions.

Fig. 5 shows a small portion of the REMPI spectrum recorded around 230 nm, using an OCS sample and monitoring the m/z 28 (CO^+) and m/z 32 (S^+) mass channels. These resonances are attributable to 2 + 1 REMPI of, respectively, ground state CO fragments (resonance enhanced by the zeropoint level of the $B^1\Sigma^+$ state) and $S(^1D)$ atoms [40]. The appearance of these fragments is wholly consistent with previous photochemical studies of OCS at these near-UV excitation wavelengths [23,38], which have shown CO(X) + $S(^1D)$ to be the dominant primary products resulting from dissociation of the (bent) $^1\Delta$ excited state and that the nascent CO(X) products have a highly excited, bimodal rotational state population distribution. In much the same way, analysis of the wavelength-resolved 1 + 1 REMPI spectrum of the $CS(a^3\Pi)$ fragments resulting from two-photon dissociation of CS_2 at wavelengths ca. 290 nm has revealed that most of the available energy is partitioned into product internal excitation [31].

3.3. Possible pitfalls

Our final example provides further illustration of the benefits of being able to record REMPI spectra with both mass selection and photoelectron kinetic energy selection. The upper panel in Fig. 6 shows the, at first sight, surprisingly complicated three-photon ionisation spectrum of a jet-cooled sample of CS_2 that is obtained following excitation in the wavelength range 356.5–347 nm whilst monitoring just that fraction of the total ion yield with TOF appropriate for m/z 76. By way of contrast, the lower panel shows how much simpler the same spectral region appears when, instead, we monitor just that fraction of the total photoelectron yield with kinetic energy in excess of 0.35 eV. The striking differences are a reflection that the former spectrum is actually a superposition of one- and two-photon resonance enhancements associated with, respectively, excitations to bent valence states (at the one-photon energy) and linear Rydberg states (at the two-photon energy). Franck–Condon requirements dictate that only

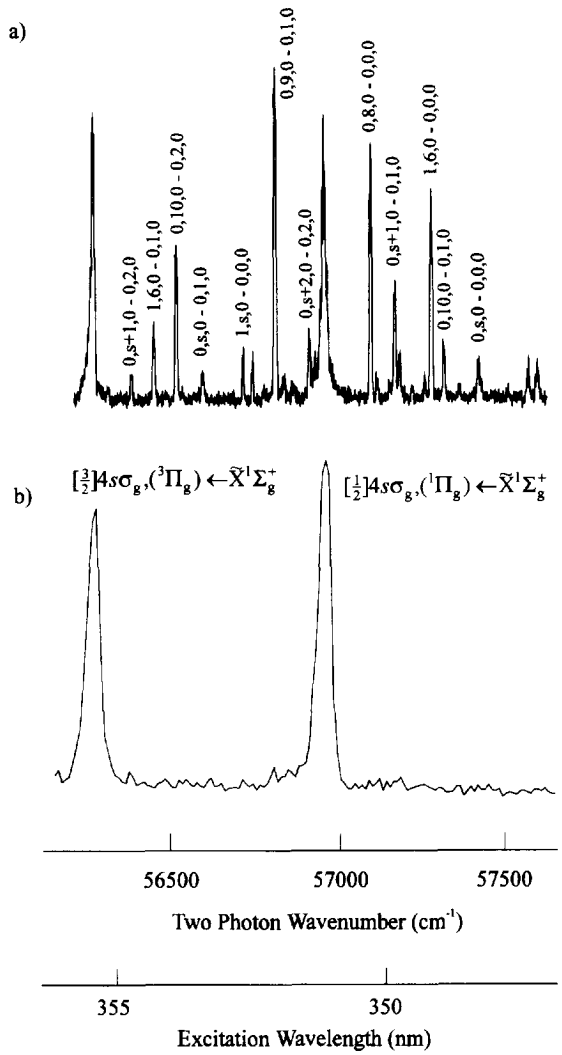

Fig. 6. Detail of part of the overall three-photon ionisation spectrum of CS_2 obtained by monitoring (a) the yield of parent ions, and (b) the yield of photoelectrons with kinetic energies greater than ca. 0.35 eV, as a function of excitation wavelength. As discussed in the text, the former spectrum (a) contains a superposition of one- and two-photon resonances associated with excitations to bent valence states and linear Rydberg states, respectively, whilst, because of the photoelectron kinetic energy chosen, only the latter contribute in spectrum (b). The vibronic assignments indicated in (a) are taken from Ref. [7].

the latter ionise to $v^+ = 0$ ions and thus give rise to photoelectrons with sufficiently high kinetic energy to contribute to the spectrum shown in Fig. 6(b). The different spectral widths of the features common to both spectra are a reflection of the broader rotational envelope associated with the near-room-temperature sample used in the REMPI–PES study. The deduced quantum defects of these two bands ($\delta \sim 1.9$, if we assume a principal quantum number, $n = 4$) are both consistent with previous assignments [30] that these two features correspond to the $[^3/_2]4s\sigma_g, (^3\Pi_g) \leftarrow \tilde{X}^1\Sigma_g^+$ and $[^1/_2]4s\sigma_g, (^1\Pi_g) \leftarrow \tilde{X}^1\Sigma_g^+$ Rydberg origins, respectively.

4. Conclusions

REMPI spectroscopy, especially when performed in conjunction with kinetic energy analysis of the accompanying photoelectrons, is now widely recognised as a very powerful technique for unravelling aspects of the spectroscopy, and in some cases the dynamics, of the excited electronic states of numerous small and medium sized polyatomic molecules. Here we have chosen to highlight aspects of recent REMPI and REMPI–PES studies of the molecules OCS and CS_2 to illustrate some of the many virtues (and a few potential limitations) of these techniques.

Acknowledgements

The Bristol group is happy to acknowledge the help, support and encouragement of Mr K.N. Rosser, and financial support from the EPSRC (previously SERC), in the form of equipment grants and a studentship (to RAM). AJO-E is grateful to the Royal Society for the award of the Eliz. Challenor Research Fellowship, whilst DA acknowledges financial support from the European Union Erasmus scheme. The Amsterdam group is grateful to the Netherlands Organisation for Scientific Research (NWO) for equipment grants and financial support.

References

[1] M.N.R. Ashfold and J. D. Howe, Ann. Rev. Phys. Chem., 45 (1994) 57 and references therein.
[2] G. Herzberg, Molecular Spectra and Molecular Structure, Vol III. Electronic Spectra and Electronic Structure of Polyatomic Molecules, Van Nostrand Reinhold, Princeton, NJ, 1966.
[3] J.W. Rabalais, J.M. McDonald, V. Scherr and S.P. McGlynn, Chem. Rev., 71 (1971) 73.
[4] S.V. Filseth, Adv. Photochem., 10 (1977) 1.
[5] M.N.R. Ashfold, M.T. Macpherson and J.P. Simons, Topics in Current Chem., 86 (1979) 1 and references therein.
[6] H. Bitto, A. Ruzicic and J.R. Huber, Chem. Phys., 189 (1994) 713 and references therein.
[7] B. Kleman, Can. J. Phys., 41 (1963) 357.
[8] I.M. Waller and J.W. Hepburn, J. Chem. Phys., 87 (1987) 3261.
[9] W.-B. Tzeng, H.-M. Yin, W.-Y. Leung, J.-Y. Luo, S. Nourbakhsh, G.D. Flesch and C.Y. Ng, J Chem. Phys., 88 (1988) 1658.
[10] S.P. Sapers and D.J. Donaldson, J Phys. Chem., 94 (1990) 8918; Chem. Phys. Lett., 198 (1992) 341.
[11] C. Starrs, M.N. Jego, A. Mank and J.W. Hepburn, J Phys. Chem., 96 (1992) 6526.
[12] J. G. Frey and P. Felder, Chem. Phys., 202 (1996) 397 and references therein.
[13] A. Mank, C. Starrs, M.N. Jego and J.W. Hepburn, J. Chem. Phys., 104 (1996) 3609.
[14] W.C. Price and D.M. Simpson, Proc. Roy. Soc., Ser. A, 165 (1938) 272.
[15] F.R. Greening and G.W. King, J. Mol. Spectrosc., 59 (1976) 312.
[16] M.-J. Hubin-Franskin, J. Delwiche, A. Poulin, B. Leclerc, P. Roy and D. Roy, J. Chem. Phys., 78 (1983) 1200 and references therein.
[17] G. Black, R.L. Sharpless and T.G. Slanger, J. Chem. Phys., 66 (1977) 2113.
[18] W.C. Price and D.M. Simpson, Proc. Roy. Soc., Ser. A, 169 (1939) 50.
[19] I. Kopp, Can. J. Phys., 45 (1967) 4011.
[20] F.M. Matsunaga and K. Watanabe, J. Chem. Phys., 46 (1967) 4457 and references therein.
[21] B. Leclerc, A. Poulin, D. Roy, M.J. Hubin-Franskin and J. Delwiche, J. Chem. Phys., 75 (1981) 5329.
[22] J.A. Joens, J. Chem. Phys., 89 (1985) 5366 and references therein.
[23] N. Sivakumar, G.E. Hall, P.L. Houston, J.W. Hepburn and I. Burak, J. Chem. Phys., 88 (1988) 3692 and references therein.
[24] C.D. Pibel, K. Ohde and K. Yamanouchi, J. Chem. Phys., 101 (1994) 836 and references therein.
[25] G. Black, R.L. Sharpless, T.G. Slanger and D.C. Lorents, J. Chem. Phys., 62 (1975) 4274.
[26] C.E. Strauss, G.C. McBane, P.L. Houston, I. Burak and J.W. Hepburn, J. Chem. Phys., 90 (1989) 5364.
[27] B. Yang, M.H. Eslami and S.L. Anderson, J. Chem. Phys., 89 (1988) 5527.
[28] R. Weinkauf and U. Boesl, J. Chem. Phys., 98 (1993) 4459.
[29] R-A. Morgan, A.J. Orr-Ewing, D. Ascenzi, M.N.R. Ashfold,

W.J. Buma, C.R. Scheper and C.A. de Lange, J. Chem. Phys., 105 (1996) 2141.
[30] S. Couris, E. Patsilinakou, M. Lotz, E.R. Grant, C. Fotakis, C.
[31] R.A. Morgan, M.A. Baldwin, A.J. Orr-Ewing, M.N.R. Ashfold, W.J. Buma, J.B. Milan and C.A. de Lange, J. Chem. Phys., 104 (1996) 6117.
[32] L. Li, X.T. Wang, X.N. Li and X.B. Xie, Chem. Phys., 164 (1992) 305; Chem. Phys. Lett., 202 (1993) 115.
[33] J. Baker, M. Konstantaki and S. Couris, J. Chem. Phys., 103 (1995) 2436.
[34] J. Baker and S. Couris, J. Chem. Phys., 103 (1995) 4847.
[35] D.P. Taylor and P.M. Johnson, J. Chem. Phys., 98 (1991) 1810 and references therein.
[36] M.R. Dobber, W.J. Buma and C.A. de Lange, J. Chem. Phys., 101 (1994) 9303.
[37] I. Fischer, A. Lochschmidt, A. Strobel, G. Niedner-Schatteburg, K. Müller-Dethlefs and V.E. Bondybey, Chem. Phys. Lett., 202 (1993) 542.
[38] Y. Sato, Y. Matsumi, M. Kawasaki, K. Tsukiyama and R. Bersohn, J. Phys. Chem., 99 (1995) 16307.
[39] L.-S. Wang, J.E. Reutt, Y.T. Lee and D.A. Shirley, J. Electron. Spectrosc. Rel. Phenom., 47 (1988) 167.
[40] S.T. Pratt, Phys. Rev. A, 38 (1988) 1270.